

Accepted Manuscript



Separating and characterizing functional alkane degraders from crude-oil-contaminated sites via magnetic nanoparticle-mediated isolation

Xinzi Wang, Xiaohui Zhao, Hanbing Li, Jianli Jia, Yueqiao Liu, Odafe Ejenavi, Aizhong Ding, Yujiao Sun, Dr. Dayi Zhang

PII: S0923-2508(16)30077-8

DOI: [10.1016/j.resmic.2016.07.004](https://doi.org/10.1016/j.resmic.2016.07.004)

Reference: RESMIC 3525

To appear in: *Research in Microbiology*

Received Date: 11 January 2016

Revised Date: 6 July 2016

Accepted Date: 8 July 2016

Please cite this article as: X. Wang, X. Zhao, H. Li, J. Jia, Y. Liu, O. Ejenavi, A. Ding, Y. Sun, D. Zhang, Separating and characterizing functional alkane degraders from crude-oil-contaminated sites via magnetic nanoparticle-mediated isolation, *Research in Microbiologoy* (2016), doi: 10.1016/j.resmic.2016.07.004.

This is a PDF file of an unedited manuscript that has been accepted for publication. As a service to our customers we are providing this early version of the manuscript. The manuscript will undergo copyediting, typesetting, and review of the resulting proof before it is published in its final form. Please note that during the production process errors may be discovered which could affect the content, and all legal disclaimers that apply to the journal pertain.

1 **For publication**

2 **Separating and characterizing functional alkane degraders**
3 **from crude-oil-contaminated sites via magnetic**
4 **nanoparticle-mediated isolation**

5 Xinzi Wang^a, Xiaohui Zhao^{a,b}, Hanbing Li^a, Jianli Jia^c, Yueqiao Liu^{a,b}, Odafe
6 Ejenavi^a, Aizhong Ding^b, Yujiao Sun^b, Dayi Zhang^{a,*}

7 ^a *Lancaster Environment Center, Lancaster University, Lancaster, LA1 4YQ, UK*

8 ^b *College of Water Sciences, Beijing Normal University, Beijing, 100875, PR China*

9 ^c *School of Chemical and Environmental Engineering, China University of Mining &*
10 *Technology (Beijing), Beijing, 100083, PR China*

11
12 Corresponding author:

13 Dr. Dayi Zhang

14 Email: d.zhang@lancaster.ac.uk

15 Telephone: +44 (0)1524 510288

16

17

18

19 **Abstract**

20 Uncultivable microorganisms account for over 99% of all species on the
21 planet, but their functions are yet not well characterized. Though many
22 cultivable degraders for n-alkanes have been intensively investigated, the roles
23 of functional n-alkane degraders remain hidden in the natural environment.
24 This study introduces the novel magnetic nanoparticle-mediated isolation (MMI)
25 technology in Nigerian soils and successfully separates functional microbes
26 belonging to the families *Oxalobacteraceae* and *Moraxellaceae*, which were
27 dominant and responsible for alkane metabolism in situ. The *alkR*-type
28 n-alkane monooxygenase genes, instead of *alkA*- or *alkP*-type, were the key
29 functional genes involved in the n-alkane degradation process. Further
30 physiological investigation via a BIOLOG PM plate revealed some carbon
31 (Tween 20, Tween 40 and Tween 80) and nitrogen (tyramine, L-glutamine and
32 D-aspartic acid) sources promoting microbial respiration and n-alkane
33 degradation. With further addition of promoter carbon or nitrogen sources, the
34 separated functional alkane degraders significantly improved n-alkane
35 biodegradation rates. This suggests that MMI is a promising technology for
36 separating functional microbes from complex microbiota, with deeper insight
37 into their ecological functions and influencing factors. The technique also
38 broadens the application of the BIOLOG PM plate for physiological research
39 on functional yet uncultivable microorganisms.

40

41 **Keywords:** n-Alkane; Soil; Biodegradation; Magnetic nanoparticle-mediated
42 isolation;Uncultivable microorganisms; Functional alkane degraders; BIOLOG
43 PM plate

44

45

46 1. Introduction

47 Many environmental hazardous chemicals have been released into the
48 environment through various industrial activities. With the industrial
49 development and urbanization process, increasing use of crude oil has
50 consequently caused numerous oil spill accidents and contaminated sites.
51 Since 1969, there have been over 40 large oil spill incidents throughout the
52 world, such as the Exxon Valdez oil spill in Prince William Sound in 1989 [1, 2],
53 the Deepwater Horizon oil spill in the Gulf of Mexico [3] and the Xingang oil spill
54 in Dalian [4] in 2010. These resulted in large areas of oil-contaminated sites,
55 affected ecological systems and threatened human health [5, 6].

56 Many microbes are involved in the natural n-alkane degradation process,
57 under either aerobic or anaerobic conditions [7-12]. The identified n-alkane
58 degraders include: *Acinetobacter* [13, 14], *Alcaligenes* [13], *Alcanivorax* [15-18],
59 *Arthrobacter* [19], *Geobacillus* [20], *Bacillus* [21, 22], *Brachybacterium* [23],
60 *Burkholderia* [24], *Desulfatibacillum* [25, 26], *Dietzia* [27, 28], *Geobacillus* [29],
61 *Gordonia* [30], *Marinobacter* [31, 32], *Mycobacterium* [33, 34], *Paracoccus* [22,
62 35], *Planococcus* [36], *Pseudomonas* [37, 38], *Rhodococcus* [34, 39, 40] and
63 *Thermooleophilum* [41]. They are widely distributed in hydrocarbon-polluted or
64 non-polluted environments, with essential roles in n-alkane degradation [42].
65 Meanwhile, alkane monooxygenases encoding genes vary widely among these
66 alkane degraders, although they all share considerable sequence homology
67 [43]. One type of *alkB* gene from *Pseudomonas* [44, 22] encodes alkane
68 monooxygenases metabolizing short- or medium-chain n-alkanes, with a
69 carbon chain length from 14 to 20. *Rhodococcus* is capable of degrading C₇ to
70 C₂₀ n-alkanes, with *alkB1/alkB2* nucleotide sequences sharing high similarity to
71 *alkB* [45-47]. In addition, *Acinetobacter* has a different *alkM* gene [48] for
72 utilizing n-alkanes from C₁₃ to C₄₄ [49, 50, 13], and its n-alkane oxidation
73 capacity is higher for medium- and long-chain alkanes [51, 52] than for
74 short-chain ones [53]. Other research also identified various alkane
75 hydroxylase genes with different sequence identities from those in pure
76 cultured strains [54, 55]. Such diverse alkane monooxygenase-encoding genes
77 involved in alkane metabolism therefore cause an underestimation of the

78 alkane biodegradation pathway in the natural environment and are attracting
79 increasing academic attention.

80 To understand the behavior of n-alkane degradation, both sequence- and
81 function-based approaches have been attempted. Sequence-based
82 techniques include denaturing gradient gel electrophoresis (DGGE), the 16S
83 rRNA clone library and metagenomics high-throughput sequencing [56]. All
84 these molecular tools provide new opportunities for interpreting and
85 the characteristics of microcosms in natural environments [57]. Lindstrom et al.
86 reported declining microbial diversity with long-term crude oil contamination
87 [58], and the relative abundance of n-alkane degraders (*Rhodococcus*,
88 *Sphingomonas* and *Pseudomonas*) was significantly increased [59]. In marine
89 sediments, oil contamination also affects microbial community structure and
90 function, consequently resulting in increased oil-metabolizing activities and
91 decreased diversity of the microbial population [60, 61]. It is also reported
92 that geographic locations determine functional or species diversity within
93 bacterial communities at oil-contaminated sites [62, 63], and
94 contamination type and history significantly affect the community and
95 population of soil microorganisms, leading to less microbial diversity and
96 functions in heavily-contaminated soils than in those with light contamination
97 [64, 65]. Function-based approaches focus on cultivation and physiological
98 behavior of n-alkane degraders or soil enzymatic activities to investigate
99 the ecological functions and responses of soil microbes to n-alkane
100 contamination [66]. For instance, *Pseudomonas* [67] and *Rhodococcus* [68]
101 are characterized as the most common cultivable n-alkane degraders in soil.
102 The correlation between microbial diversity degradation and their physiological
103 functions in crude-oil-contaminated soils has been successfully explained by
104 the BIOLOG phenotype assay [58]. The dynamics of the soil microbial
105 population, community composition and enzymatic activities also reveal the
106 response of the microbial community to crude oil contamination during the
107 degradation process [69-72]. By directly analyzing the functions and
108 phenotypic behavior of alkane degraders, bioaugmentation and biostimulation
109 have been applied as cost-effective and environmentally friendly methods to
110 improve the biodegradation performance by adding exogenous degrading
111 strains or growth substrates [73-77], such as electron acceptors (oxygen

112 supply) and nutrients (nitrogen and phosphorus substrates) [78-82].
113 Most microorganisms (>99%) are uncultivable under laboratorial conditions,
114 but functional in natural environments [83]. They play key roles in the
115 natural carbon and nitrogen cycle but their physiology is hard to investigate,
116 especially that of the n-alkane degraders. It is a great challenge when using
117 traditional function- or sequence-based approaches to reveal the in situ
118 ecological functions of uncultivable microorganisms, where
119 function-based cultivation cannot effectively isolate these microbes, and the
120 sequence-based method is unpredictable due to a huge database without
121 accurate allocation of their functions. Stable isotope probing (SIP) is a
122 promising technique investigating functional-yet-uncultivable microbes [84].
123 The biomass (DNA, RNA or protein) of the functional-yet-uncultivable microbes
124 becomes heavier during the metabolism of stable isotope-labeled substrates
125 (^{13}C or ^{15}N), and can then be further separated by the difference in buoyant
126 density [84]. Numerous degraders of phenolic compounds and polycyclic
127 aromatic hydrocarbon (PAHs) have been identified via SIP in
128 crude-oil-contaminated sites, including *Burkholderia*, *Alcanivorax* and
129 *Cycloclasticus* [85, 86]. Nevertheless, SIP is a challenge, since the
130 ^{13}C -labeled substrate is very expensive and the dosage is normally single pure
131 chemicals instead of mixtures [87]. In most environmental degradation
132 cases, multi-contaminants exist at the contaminated sites. Particularly for
133 alkane degradation, the complicity of n-alkane composition in the natural
134 environment strongly restricts the applicable feasibility of SIP.
135 Magnetic-nanoparticle-mediated isolation (MMI) is a recently developed
136 method for separating living functional microbes from complex microbiota [88].
137 After being functionalized with magnetic nanoparticles (MNPs) and dosed with
138 targeted carbon sources, the living active degraders gradually divide and
139 ultimately lose their magnetic attraction, whereas inert bacteria remain
140 silent and their magnetism is constant [88, 89]. Therefore, functional microbes
141 can be effectively be separated by magnetic fields from the whole microbiota.
142 In this way, the MMI technique does not rely on substrate labeling and can be
143 used in microcosms with multiple carbon or nitrogen sources. More importantly,
144 the separated bacterial cells are still alive and suitable for further physiological
145 investigation, providing more comprehensive information on microbial diversity

146 and ecological functions.

147 To address these challenges, this research aims to develop a new method
148 investigating functional n-alkane degraders in the natural soil microcosm,
149 with n-alkane mixtures as carbon sources. Via magnetic separation of living
150 n-alkane degraders, the present study focused on their phenotype and
151 n-alkane degradation performance by the BIOLOG PM plate. To the best of our
152 knowledge, this is the first successful identification of functional
153 n-alkane degraders from soils that reveals their phenotypic behavior and the
154 enhancing of n-alkane degradation efficiency with the addition of extra nitrogen
155 sources.

156

157 **2. Materials and methods**

158 *2.1. Contaminated site and sample collection*

159 The crude-oil-contaminated site is located in Delta State, Nigeria (N
160 7°15'16.9", E 4°41'23.95"). Five national crude oil drilling wells are distributed
161 within 5 km of the site and there have been intensive oil exploration activities
162 since the 1980s. With a long history of crude oil contamination caused by
163 drilling wells and pipeline spillages, severe cases of crude oil contamination
164 have been observed, and the average n-alkane content in the research area is
165 about 2.0% (w/w). The soil samples were collected on June 14, 2015. During
166 the collection, the surface soils (0-10 cm) were gently removed to avoid the
167 impact of human activities and disturbance. A total of 500 grams of soils
168 from a depth of 10-20 cm were collected, sieved to remove plant debris and
169 stones and finally stored at 4°C before further analysis.

170 *2.2. MNP synthesis and targeting of soil functionalization*

171 The synthesis of MNPs followed previous instructions [90]. One mL
172 FeCl₂ (1.0 M) and 2 mL FeCl₃ (2.0 M) were gently mixed, with further
173 drop-by-drop addition of 25 mL NaOH (2.0 M). After continuous shaking for 30
174 min, the synthesized dark nanoparticles were harvested by a magnet for 10
175 min and washed by 30 mL deionized water several times until neutral pH
176 value (7.0). The synthesized MNPs concentration was 9.1 g/L.

177 To test the soil magnetic functionalization efficiency and optimize soil
178 magnetism for effective separation, 1.0 mL synthesized MNPs were mixed

179 with soils of weights from 0.06 mg to 17,700 mg. After gently shaking for 5 min,
180 the magnetic functionalized soils were harvested by a permanent magnet for
181 10 min. A quantitative polymerase chain reaction (qPCR) was used to quantify
182 the bacterial concentration in the supernatant (bacterial 16S rRNA copy
183 numbers in magnetic-free fraction, BC_{MF} for short, copies/mL) and magnetic
184 soil pellet (BC_{MS} , copies/mL). The soil magnetic functionalization efficiency
185 was calculated as the ratio of the bacterial amount in magnetic soil pellet to the
186 total amount ($BC_{MS}/(BC_{MF}+BC_{MS})$). Here, 100% soil magnetic functionalization
187 efficiency indicates that all soil bacteria are successfully magnetically
188 functionalized ($BC_{MF}=0$ copies/mL), and 0% refers to no soil bacteria with
189 magnetism ($BC_{MS}=0$ copies/mL).

190 From the curve of soil magnetic functionalization efficiency (Fig. 1), the
191 MNP-functionalized soil samples were prepared by mixing 500 mg soil (dry
192 weight) and 0.91 mg MNPs as the optimal condition for n-alkane
193 biodegradation treatments.

194 *2.3. Alkane biodegradation treatments*

195 For n-alkane biodegradation, soil samples were spiked with/without 2%
196 (w/w) mineral oil (Sigma Aldrich, UK) and mixed well. The five treatments
197 included $HgCl_2$ (0.1%)-treated soils with mineral oil (sterile control), original
198 soils without mineral oil (CKN), original soils with mineral oil amendment (CKP),
199 MNP-functionalized soils without mineral oil amendment (MNPN) and
200 MNP-functionalized soils with mineral oil amendment (MNPP). All
201 treatments were carried out in biological triplicates and the microcosms were
202 incubated at room temperature for 40 days. Around 2.0 g of soils were
203 collected on days 5, 10, 20, 30 and 40 for chemical and biological analysis
204 directly in CKN and CKP treatments. To evaluate the in situ phenotype of
205 separated n-alkane degraders in MNPN and MNPP treatments, we prepared
206 the sterile soil extraction solution by adding 1.0 g original soils in 10 mL
207 deionized water and passing through a 0.45 μ m filter. The 0.45 μ m filter aimed
208 to remove most of the soil particles and living bacterial cells in the soil
209 suspension. Some small bacterial cells might still remain in the aqueous phase,
210 but their impact on oil degradation was minimal from our BIOLOG tests. To
211 separate magnetic-free cells (MFCs), 2.0 g of soil samples from MNPN

212 and MNPP treatments at each sampling time point were further suspended in
213 the sterile soil extraction solution and the MFCs were separated from the
214 inert microbes (magnetic pellets) by a magnet and marked as MFCN for
215 MNPN treatment and MFCP for MNPP treatment.

216 2.4. DNA extraction, amplification and sequencing

217 The soil and MFC DNA was extracted via a PowerSoil DNA extraction kit
218 (MOBIO, USA) in accordance with the manufacturer's instruction. Targeting
219 DNA was amplified by the polymerase chain reaction (PCR). The primer pairs
220 and PCR program for 16S rRNA- and n-alkane-degrading functional genes are
221 listed in Table 1 [91-94]. The three pairs of primers for n-alkane
222 monooxygenase genes (*alk_A*, *alk_P* and *alk_R*) were used to characterize
223 the diversity of *alkB* genes and link them to n-alkane degraders (*Acinetobacter*,
224 *Pseudomonas* and *Rhodococcus*, respectively) in soil following previous
225 protocols [43]. These three types of *alkB* genes shared considerable sequence
226 homology, but varied in different species with phylotypic differences [43]. The
227 50 μ L PCR reaction system contained 2 μ L deoxynucleotide triphosphates
228 (dNTPs, 5 mM), 2 μ L of each primer (5 mM), 1 μ L DNA template, 0.3 μ L Dream
229 Taq DNA polymerase (Fermentas, UK) and 37.7 μ L ultrapure water (molecular
230 biology grade, Sigma Aldrich, UK).

231 Quantification of 16S rRNA and n-alkane monooxygenase genes (*alk_A*,
232 *alk_P* and *alk_R*) was determined by qPCR. The 20 μ L qPCR system
233 consisted of 2 μ L of each primer, 1 μ L DNA template, 5 μ L ultrapure water and
234 10 μ L iTaq™ Universal SYBR® Green Supermix (BioRad, USA). Standard
235 curves were obtained with serial dilutions of quantified plasmid DNA (via
236 nanodrop) containing the fragment of 16S rRNA and *alkB* genes. The qPCR
237 programs were the same as the PCR programs above except for the extra
238 fluorescence data acquisition at 80°C for 15 s in each cycle.

239 To determine microbial community structure in soils and MFCs, the
240 extracted DNA was sequenced with PCR amplicon libraries of the
241 hypervariable V3, V4 and V6 region of the 16S rRNA genes (Annoroad Gene
242 Technology Co., Ltd, Beijing, China.). Pyrosequencing was carried out by an
243 Illumina HiSeq4000 with an average read length of 450 bp after PEAR
244 alignment [95]. All reads passed quality filtering and the reads were

245 discarded if the bar codes were uncorrectable, the bases with a Phred Quality
246 score <19 covered over 30% of the read or the ambiguous bases were over
247 5%. Sequences were assigned to operational taxonomic units (OTUs) with
248 97% pairwise identity as the threshold, and then classified taxonomically by
249 the Greengenes 16S rRNA reference database. The distance matrices from
250 samples were generated by the Bray-Curtis metric and visualized by principal
251 coordinates analysis (PCoA) by QIIME (Quantitative Insights Into Microbial
252 Ecology) software.

253 2.5. Community substrate utilization analyses

254 BIOLOG PM plates (BIOLOG, USA) were used to examine the carbon and
255 nitrogen metabolisms of MFCs from MNPP and MNPN treatments. The 150 μ L
256 of MFCs were added to each well of PM01 (95 carbon sources) and PM03
257 (95 nitrogen sources with additional 500 mg/L mineral oil as the sole carbon
258 source), supplemented with 1.5 μ L BIOLOG Redox Dye Mix A (100 \times). The
259 plates were incubated at 25°C for 48 h and color development was read
260 every 15 min as absorbance at 590 nm wavelength by a multimode microplate
261 reader (FLUOstar Omega, BMG Labtech, UK) [96]. The data were collected
262 and further analyzed by MARS software (BMG Labtech, UK).

263 2.6. n-Alkane chemical analyses

264 Determination of n-alkane content in soils followed the hexane extraction
265 method. All soil samples were freeze-dried and each gram of soil was
266 spiked with 1 mL 5 α -cholestane as a surrogate standard. Added to 10 mL
267 hexane, the soil-hexane mixture was ultrasonically homogenized for 2 min (40
268 kHz) and the supernatant was further fractionalized by column
269 chromatography [97]. The glass column (Φ 10 mm \times 100 mm) consisted of 2
270 cm anhydrous Al₂O₃ and 0.3 cm anhydrous Na₂SO₄ from the bottom to the top.
271 Pre-washed with hexane, the column was loaded with soil-hexane
272 supernatants and washed with 20 mL of hexane. The collection was then
273 evaporated in a 40°C water bath and re-dissolved in 1.0 mL hexane. The
274 internal standard solution was tetracosane (C₂₄D₅₀) at 50 mg/L [98].

275 Analysis of the extracts was carried out using a gas chromatography flame
276 ionization detector (GC-FID). One μ L of sample was injected into a Hewlett
277 Packard gas chromatograph GC 5890 coupled with a 5971A flame ionization

278 detector. The GC was equipped with a capillary column DB 5MS (60 m × 0.2
279 mm × 0.32 μm, J&W Scientific). The temperature program was set as 1 min at
280 35°C, followed by a progressive increase to 310°C at a rate of 10°C/min, and
281 finally, 10 min at 310°C.

282 For n-alkane residues in the BIOLOG PM assay, there was a technical
283 problem in our lab when applying hexane extraction for high-throughput
284 extracting and analyzing alkanes in a small volume of water sample in each
285 well (150 μL). We therefore used alkane whole-cell bioreporter ADPWH_alk
286 [99] to detect n-alkane concentrations after degradation. This alkane
287 bioreporter had a detection range from 0.1 mg/L to 100 mg/L [99, 100], with
288 similar sensitivity to GC-FID and that fit well with the n-alkane dosage in this
289 study. After cultivation in lysogeny broth medium at 30°C overnight,
290 ADPWH_alk bioreporter cells were washed by deionized water and
291 resuspended in minimal medium with 20 mM sodium succinate as sole
292 carbon source [4, 99]. The 50 μL solution from each well of BIOLOG PM03 (95
293 nitrogen sources) was mixed with 150 μL ADPWH_alk suspension, and added
294 to the wells of 96-well black and clear-bottom microplate (Corning, USA) with
295 three replicates. This was incubated at 30°C for 6 h and the bioluminescent
296 signal was measured every 10 min using the FLUOstar Omega microplate
297 reader. Induced bioluminescence was calculated by the average of
298 bioluminescent measurements between 180 and 210 min. The
299 bioluminescence response ratio was calculated by dividing the induced
300 bioluminescence by the original bioluminescence (time = 0 min), and the
301 relative bioluminescence response ratio was calculated by dividing the induced
302 bioluminescence (samples) by that of the control (non-induced). The residual
303 n-alkane concentration was evaluated by the gene expression model [101, 102]
304 and the calibration curve [99] as described previously.

305 *2.7. Statistical analysis*

306 All statistical calculations were performed by SPSS 17.0. One-way
307 ANOVA and least significant difference (LSD) tests were employed in
308 analysis of the statistical significance of differences and variance
309 (p -value<0.05) of n-alkane residuals and 16S/alkane-monooxygenase gene
310 copy numbers in different treatments. Correlation analysis between the

311 microbial respiration level and the n-alkane degradation rate was conducted
312 with a significant level of less than 0.05.

313

314 **3. Results and discussion**

315 *3.1. Optimal condition of soil microcosm functionalization with MNPs*

316 Both soil microorganisms and particles are predominantly negatively
317 charged, resulting in the strong electrostatic interaction with positively charged
318 MNPs [103]. This study investigated the optimal weight ratio of soil to MNPs
319 (ranging from 0.066 to 19,500, w/w) to achieve both high magnetic
320 functionalization efficiency and minimal MNP dosages. The residual bacterial
321 counts were quantified by qPCR, and Fig. 1 shows that magnetic
322 functionalization efficiency was maintained at over 99.5% when the ratio of soil
323 to MNPs was less than 1,100 (w/w). Beyond the critical point, the magnetic
324 functionalization efficiency dramatically declined to only 90.88%
325 (soil:MNPs=5,300, w/w) and 16.65% (soil:MNPs=19,500, w/w), due to
326 excessive negative soil particles or bacterial cells in the system. The
327 functionalization of bacterial cells by MNPs was attributed to the electrostatic
328 interaction between MNPs and carboxyl(-COOH)/thiol(-SH)/amine(-NH₂)
329 functional groups on the bacterial cell membrane [104, 105]. Since these
330 functional groups are universal for all bacterial cells, the non-selective
331 adhesion mechanism ensures that all bacterial cells can be effectively
332 functionalized with magnetism. The optimal condition for further n-alkane
333 biodegradation treatment was therefore set at 500 mg soil (dry weight) and
334 0.91 mg MNPs (0.1 mL suspension).

335 *3.2. The degradation of n-alkanes in soils*

336 After 40 days of incubation, the n-alkanes were significantly degraded by
337 soil microbes, as illustrated in Fig. 2(A). The concentration of n-alkanes showed
338 a slight decrease (<83%) with time in the sterile control, whereas significantly
339 higher degradation efficiencies were achieved in all n-alkane-amended
340 treatments (CKP and MNPP, *p*-value <0.05). There was no significant
341 difference between n-alkane degradation rates in soils with/without MNP
342 functionalization (MNPP and CKP, *p*-value<0.05), indicating that MNPs did not
343 affect bacterial activities or the n-alkane degradation performance [88].

344 Dramatic n-alkane degradation was observed in the first 20 days, when
345 n-alkane degradation efficiency was 68.6% and 80.7% in CKP and MNPP
346 treatments, respectively. Afterwards, n-alkane degradation was slowed down
347 and n-alkane degradation efficiency achieved 90.7% and 83.4% in CKP and
348 MNPP treatments, respectively, after 40 days of degradation. The results of
349 GC-FID (Fig. 2(B)) illustrated the change in individual n-alkanes with specific
350 carbon chain length. In the sterile control, C₁₀ and C₁₁ alkanes had the lowest
351 residual ratio (30.9% and 46.2%) due to their higher vapor pressure. About
352 70%-90% of C₁₂-C₁₅ medium-chain alkanes and over 90% of alkanes with
353 carbon chain length >16 remained in the soil. For both CKP and MNPP
354 treatments, the removal efficiency for short-, medium- and long-chain alkanes
355 were 81.2%-88.5%, 68.3%-77.4% and 40.1%-68.4%, respectively. The short-
356 and medium-chain alkanes have higher solubility and degradation rates than
357 long-chain alkanes [106, 107], and they might favor bacterial metabolism.
358 Therefore, the slower alkane degradation rates after 20 days might possibly be
359 attributed to declining alkane solubility and degradation rates in soils. Our
360 results were similar to previous research on aerobic alkane biodegradation
361 [108], but significantly higher than anaerobic alkane degradation [109, 110].
362 From the n-alkane biodegradation curve, the soil DNA was extracted on day 20
363 and day 40, representing rapid and slow degradation steps, to address the
364 respective profiles of microbial community structure and ecological functions.

365 *3.3. The microbial community responsible for n-alkane degradation*

366 Bar-coded pyrosequencing generated 220,584 quality sequences from the
367 13 samples, from 13,066 sequences in MFCP_40 to 29,231 reads in MFCN_20.
368 At the 97% similarity level, a total of 2,176 phylotypes were defined. The
369 original soil sample (NC) and samples without n-alkane addition (CKN_20,
370 CKN_40, MNPN_20 and MNPN_40) had the highest number of phylotypes
371 detected, from 1,122 to 1,244. The phylotypes in samples with n-alkane
372 degradation were significantly lower (from 1,045 in CKP_40 to 739 in
373 MFCP_40). Significant declining alpha diversity was observed during the
374 n-alkane degradation process, wherein the Shannon-index ranged from 7.8-8.2
375 in original soil samples (NC) or those without n-alkane amendment (CKN_20,
376 CKN_40, MNPN_20 and MNPN_40) to 6.4 in soils with n-alkane degradation

377 after 40 days (CKP_40), and as low as 5.8 in the MFC fractions with
378 n-alkane degradation (MFCP_20 and MFCP_40). Our results fitted well with
379 previous findings showing that microbial diversity and functions declined
380 after n-alkane contamination and during the bioremediation process that
381 followed [60, 61, 64].

382 Cluster analysis of the relative abundance of bacteria at the family level
383 was illustrated in Fig. 3(A), representing microbial diversity in soil
384 samples amended with/without n-alkane at different time points. Of all
385 classifiable sequences, 25 phylotypes were the most dominant at the family
386 level and accounted for over 70% of all sequences. In original soil (NC), the
387 key microbes belonged to the families *Nitrospiraceae* (10.3%), *Ellin515* (7.8%),
388 *Solibacteraceae* (5.6%), *Syntrophobacteraceae* (5.2%) and *Koribacteraceae*
389 (4.8%). They were all soil microorganisms with essential roles in soil carbon
390 and nitrogen cycling. There was no significant difference between CKN and
391 MNPN treatments (p -value<0.05), indicating no microbial community change
392 in the soils with or without MNP functionalization. Thus, MNP
393 functionalization did not change soil microbial activities or community structure,
394 consistent with previous findings [88]. In treatments without n-alkanes
395 addition (CKN_20, CKN_40, MNPN_20 and MNPN_40), a similar microbial
396 community structure was observed, showing the constant microbial diversity
397 and population throughout the experiment without n-alkane amendment.
398 These five treatments were therefore within close distance to the Bray-Curtis
399 analysis (Fig. 3(B)). Directly amended with n-alkanes, the bacterial community
400 composition gradually changed and the dominant microbes in CKP_40 (40
401 days n-alkane degradation) belonged to *Moraxellaceae* (13.5%) and
402 *Bdellovibrionaceae* (6.2%). *Moraxellaceae* is a common cultivable soil microbe
403 family with the capability of n-alkane metabolism. *Bdellovibrionaceae* was also
404 previously reported with *alkB* alkane monooxygenase after the oil spill in the
405 Mexico Gulf [111]. Our results indicated that they were the cultivable n-alkane
406 degraders in the targeted soils.

407 It is quite interesting that the microbial diversity of magnetic microbes in
408 soils with MNP functionalization and n-alkane amendment (MNPP_20 and
409 MNPP_40) were similar to CKN_20 and CKN_40 (Fig. 3(A)). Meanwhile, an
410 entirely different microcosm structure was identified in MFCs, which contained

411 phylotypes belonging to the families *Oxalobacteraceae* (47.6%),
412 *Xanthomonadaceae* (8.6%), *Comamonadaceae* (5.8%) and *Brucellaceae*
413 (5.2%) in MFCP_20 treatment, and *Moraxellaceae* (28.6%) and
414 *Comamonadaceae* (14.6%) in MFCP_40 treatment. All these microbes have
415 been previously reported to have the capacity of metabolizing n-alkanes from
416 diversity analysis or direct cultivation of soil communities [112-114]. For the
417 first time, in this study, we successfully separated these living functional
418 n-alkane degraders using a cultivation-independent approach. Our results
419 show that active n-alkane degraders gradually lost magnetism due to
420 division and remained in MFC fractions. Meanwhile, the remaining microbes
421 in soil microcosm (MNPP_20 and MNPP_40) could not metabolize n-alkanes
422 and maintained magnetism, and they were therefore effectively captured by
423 the permanent magnet and separated from MFC fractions. Their community
424 diversity therefore remained stable and similar to the control. Based on the
425 difference between MFCP_20 and MFCP_40, it is suggested that, during the
426 first 20 days of the fast degradation process, identified *Oxalobacteraceae*
427 were the key functional n-alkane degraders, followed by the metabolisms of
428 *Moraxellaceae* from day 20 to day 40. Considering the change in individual
429 n-alkanes with specific carbon chain length (Fig. 2(B)), *Oxalobacteraceae*
430 hypothetically had preferential utilization of short- and medium-chain
431 alkanes, whereas *Moraxellaceae* might be capable of metabolizing long-chain
432 alkanes. PCoA results in Fig. 3(C) provide further evidence that MFCP_40
433 and CKP_40 were of different community structure, both separated from the
434 other MFC fractions (MFCN_20, MFCN_40 and MFCP_20) and the inert soil
435 samples (NC, CKN_20, CKN_40, MNPN_20, MNPN40, MNPP_20, MNPP40
436 and CKP_40).

437 3.4. Dynamics of 16S rRNA and n-alkane monooxygenase genes

438 The copy numbers of 16S rRNA and n-alkane monooxygenase genes
439 were estimated by qPCR and illustrated in Fig. 4. Throughout the n-alkane
440 degradation process, the relative abundances of 16S rRNA in CKN, CKP,
441 MNPN and MNPP samples were identical and remained at the same level
442 without significant differences (Fig. 4(A), 4.48×10^8 - 7.40×10^8 copies/mL,
443 p -value>0.05). The 16S rRNA copy numbers of MFCs from MNPN and

444 MNPP treatments were similar on day 0, ranging from 5.47×10^5 - 7.41×10^5
445 copies/mL, accounting for less than 1/1,000 of total soil microorganisms. In
446 MFCs from MNPN treatment, there was no significant difference in the
447 abundance of 16S rRNA during cultivation without n-alkane (7.41×10^5 -
448 9.64×10^5 copies/mL, p -value>0.05). Results indicated that only a limited
449 number of microorganisms could utilize soil residual carbon sources, divide
450 and lose magnetism. With n-alkane additives in MNPP treatments, 16S
451 rRNA abundance increased to 2.11×10^6 copies/mL on day 20 and 7.89×10^6
452 copies/mL on day 40, showing the growth and dominance of functional
453 n-alkane degraders in MFC fractions.

454 The relative abundance of three n-alkane monooxygenase-encoding
455 genes (*alkA*-, *alkP*- and *alkR*-type) behaved differently during the n-alkane
456 degradation process. On day 20 and day 40, *alkA*-type genes were
457 significantly higher in CKP treatment than those in CKN treatment (Fig. 4(B),
458 p -value<0.05). Compared to the MFCN fraction, they also increased in MFCP
459 fraction but only 0.88 (day 20) and 2.0 (day 40) times higher, showing their
460 limited roles in n-alkane metabolism. Throughout n-alkane biodegradation,
461 there was no significant difference in the *alkP*-type alkane monooxygenase
462 genes in any of the treatments (p -value>0.05, Fig. 4(C)). The results indicated
463 that microbes with *alkP*-type genes had minimal impact on n-alkane
464 degradation, and they were not the key functional n-alkane degraders in the
465 microcosm. Interestingly, *alkR*-type n-alkane monooxygenase genes
466 increased significantly and became more predominant in the MFC fraction
467 from MNPP treatment (MFCP), as illustrated in Fig. 4(D). Their relative
468 abundance was 123 and 48 times higher in MFCP on day 20 and day 40 than
469 those in MFCN. The addition of n-alkanes as the sole carbon source clearly
470 encouraged the growth of microbes with *alkR*-type genes, and they therefore
471 participated in the n-alkane biodegradation process. In contrast, the relative
472 abundance of *alkR*-type genes was not significantly increased in CKP and
473 MNPP treatments, compared to CKN and MNPN treatments accordingly. This
474 was explained by the rare abundance of functional n-alkane degraders with
475 *alkR*-type genes (around 1.0×10^{-13} copies per 16S rRNA copy) in the original
476 soil microcosm. Their abundance change was not as significant as that in

477 MFCs, where only functional n-alkane degraders were enriched and
478 separated.

479 Most research on n-alkane degraders in the soil microbial community
480 has addressed the cultivation of n-alkane degraders [22] or direct
481 pyrosequencing and qPCR to analyze the change in community structure and
482 functional gene abundance. The cultivable n-alkane degraders can only
483 effectively metabolize n-alkane under artificial conditions, whereas true
484 functional n-alkane degraders have rare abundance in the microbial
485 community, and their change is barely distinguished by a normal
486 pyrosequencing approach. In the present study, *Oxalobacteraceae* and
487 *Moraxellaceae* were identified as the dominant microbes in the MFC fraction
488 with n-alkane as the sole carbon source, and their
489 alkane-monooxygenase-encoding genes had high similarity to those of *alkA*-
490 and *alkR*-types [43], respectively. Thus, the significant increase in *alkA*-type
491 genes in CKP and MFCP treatments fit well with our microbial community
492 analysis, and their enrichment was attributed to the dominance of
493 *Moraxellaceae*. However, the functional *alkR*-type n-alkane monooxygenase
494 genes (belonging to *Oxalobacteraceae*) were only enriched in the MFC
495 fraction, but not CKP treatment. Results suggested that direct
496 pyrosequencing and qPCR of alkane monooxygenase genes might be
497 misleading us to conclude that only microbes with *alkA*-type genes are
498 key n-alkane degraders in situ. Our separation provided more details on the
499 alkane oxidation functional gene dynamics and the MFCs fractions had a
500 higher resolution of quantifying both *alkA*- and *alkR*-type genes due to the
501 enrichment of functional microbes. The unexpectedly high abundance of
502 *alkR*-type, particularly in MFCP_40 treatment, was not consistent with the
503 relative abundance of *Oxalobacteraceae*. Phylogenetically widespread and
504 genetic mobility of the *alkB* gene is supported by previous studies [115, 116].
505 Here, we make a similar hypothesis that horizontal gene transfer occurred and
506 that the *alkR*-type n-alkane monooxygenase genes were widespread within
507 the soil community.

508 *3.5. Phenotypic analysis of separated functional n-alkane degraders*

509 The sequence-based approach only identifies genetic information on
510 n-alkane degraders, with lack of phenotypic evidence to directly link microbial
511 functions to their identity or solutions providing more information on
512 practical implementation of n-alkane biodegradation. In contrast to direct
513 pyrosequencing of microbial community structure in soils, our MMI technique
514 has an attractive advantage in that separated functional n-alkane degraders
515 are still alive and suitable for further ecophysiological analysis. Both BIOLOG
516 high-throughput phenotypic PM01 (carbon sources) and PM03 (nitrogen
517 sources) plates were employed in this study to characterize phenotypes of
518 separated functional n-alkane degraders and identify key nitrogen sources
519 that might encourage n-alkane biodegradation performance.

520 MFCs from MNPN and MNPP treatment showed different phenotypic
521 patterns for carbon or nitrogen metabolism (Fig. 5). Here, the y-axis
522 represented the 95 carbon or nitrogen sources and the x-axis represented the
523 cultivation time (hours). The shading color changed from light dark to purple,
524 responsive to the respiration level from 0.0 to 3.5 (PM01 plate) and 0.0 to 1.5
525 (PM03 plate). The results of carbon metabolism provided evidence that
526 microbes separated via the MMI technique from MNPN and MNPP treatments
527 were not identical, and this was explained by the addition of n-alkane in MNPP
528 treatment and the enrichment of n-alkane degraders in the MFC fraction. The
529 MFCs from MNPN treatments could effectively utilize 32 carbon sources (Fig.
530 5A), 21 of which were able to be utilized by MFCs from MNPP treatment as
531 well (Fig. 5B). In addition to fumaric acid and mucic acid, MFCs from MNPP
532 treatment gave a stronger metabolism performance on Tween 20, Tween 40
533 and Tween 80. The three carbon sources have a similar structure of
534 polyoxyethylene sorbitan, but consist of different hydrophobes of laurate
535 (Tween 20), palmitate (Tween 40) and oleate (Tween 80). It was therefore
536 strongly hypothetical that the separated functional n-alkane degraders could
537 possess active lipases and their activities will be further investigated in our
538 future work.

539 To examine the effects of various nitrogen sources on the n-alkane
540 degradation rate, the sterile soil extraction solution with 500 mg/L n-alkane

541 was used in the PM03 plate for the MFCs from MNPN and MNPP treatments.
542 Fig. 5(C) and (D) illustrated their different microbial respiration profiles. It was
543 evident that only three nitrogen sources could promote microbial respiration
544 in MFCN, i.e. b-phenylethylamine, tyramine and n-acetyl-D-glucosamine,
545 whereas their n-alkane degradation rate was less than 5%. Without n-alkane
546 addition, the separated MFCN had minimal bacterial cell numbers from
547 qPCR results, and they were not responsible for n-alkane degradation.
548 Microbial respiration might result from the metabolism of residual soil carbon
549 sources or cell debris instead of utilizing n-alkanes. For the MFCP, the seven
550 nitrogen sources that improved respiration levels included L-phenylalanine,
551 D-serine, b-phenylethylamine, tyramine, glucuronamide, DL-lactamide and
552 n-acetyl-D-glucosamine. With these nitrogen sources, the n-alkane
553 degradation rates were all above 10%. Accordingly, there were ten nitrogen
554 sources promoting n-alkane degradation, with the degradation rate over
555 20% within 48 h, including L-glutamine, L-histidine, L-phenylalanine, L-proline,
556 D-aspartic acid, tyramine, glucuronamide, n-acetyl-D-glucosamine, thymine
557 and xanthine. In particular, the highest n-alkane degradation rate was
558 achieved with the addition of tyramine (43.6%), L-glutamine (42.2%) and
559 D-aspartic acid (38.2%). Based on increasing microbial respiration and the
560 n-alkane degradation rate, tyramine was suggested to be the best promoting
561 nitrogen source to encourage in situ n-alkane biodegradation.

562 Further correlation analysis between microbial respiration and the
563 n-alkane degradation rate helped further our understanding of the role of
564 nitrogen sources in the n-alkane metabolism of functional alkane degraders.
565 The Pearson correlation coefficient was 0.781 (p -value <0.001) between
566 microbial respiration and n-alkane degradation rates in MFCs from MNPP
567 treatment (red circle in Fig. 6). Results showed that separated living
568 microorganisms in MFCs after n-alkane addition were indeed functional
569 n-alkane degraders in situ. There was only a weak relationship (Pearson
570 correlation coefficient = 0.335, p -value <0.001) between the n-alkane
571 degradation rate and the microbial respiration level in MFCs from MNPN
572 treatment (white circle in Fig. 6), indicating that they were not predominantly
573 alkane degraders.

574 Numerous previous research has attempted to improve alkane
575 biodegradation by adding exogenous degrading strains, and some of them
576 have achieved good alkane degradation performances in liquid culture [117]
577 and in situ [118, 119, 73]. However, additive exogenous strains might
578 compete with indigenous microbes or be affected by soil properties, resulting
579 in the fact that the performance of bioaugmentation or biostimulation is not
580 always satisfied in the complex soil matrix [120]. The risk of species invasion
581 also requires attention due to microhabitat alterations in the soil
582 environment [121]. Meanwhile, the amendment of growth-promoting
583 substrates for stimulating indigenous alkane degraders mainly addressed
584 simple inorganic/organic nitrogen sources such as NH_4NO_3 [108, 122],
585 NaNO_3 [123], $(\text{NH}_4)_2\text{SO}_4$ [73, 124], urea [125], yeast extract [126] and
586 lipophilic fertilizers [127]. In the present study, it was interesting to note that
587 these commonly used nitrogen sources, like nitrate (A4) and urea (A5) in the
588 PM03 plate, could not encourage microbial respiration or the n-alkane
589 degradation rate, indicating that traditional nutrient additives in bioremediation
590 processes cannot effectively accelerate n-alkane degradation. A
591 high-throughput nutrient screening method is therefore recommended for
592 improving the bioremediation performance at n-alkane and
593 crude-oil-contaminated sites, relying on the effective separation of functional
594 n-alkane degraders and phenotypic characterization.

595

596 In conclusion, we have developed a modified magnetic
597 nanoparticle-mediated isolation (MMI) method in this study. For the first time,
598 this work successfully revealed both genetic information and phenotypic
599 behavior of functional n-alkane degraders in soil microcosms. The consistency
600 of phylotypes and n-alkane monooxygenase genes proved that the separated
601 *Oxalobacteraceae* and *Moraxellaceae* were the true functional n-alkane
602 degraders in situ at different n-alkane metabolism steps. From the
603 physiological study of the functional n-alkane degraders via the BIOLOG PM
604 plate, we suggest tyramine as being the promoting nitrogen source to
605 stimulate indigenous n-alkane degraders and accelerate the bioremediation
606 process. This novel technique opens a new pathway to characterizing the

607 mechanisms of n-alkane attenuation and influencing factors in the
608 biodegradation process, with great potential in crude oil bioremediation
609 enhancement and organic contaminated site management.

610

611 **Acknowledgements**

612 The authors are grateful for financial support from the National Natural
613 Science Foundation of China (41301331), the Department of Petroleum
614 Resources (DPR, Nigeria), the Petroleum Technology Development Fund
615 (PTDF, Nigeria) and a Lancaster University FST research grant. Annoroad
616 Gene Technology Co. Ltd (Beijing, China) helped in 16S rRNA sequence and
617 data analysis.

618

619

620 **References**

- 621 [1] Bence AE, Kvenvolden KA, Kennicutt MC. Organic geochemistry applied to
622 environmental assessments of Prince William Sound, Alaska, after the Exxon
623 Valdez oil spill - A review. *Org. Geochem.* 1996;24:7-42.
- 624 [2] Bragg JR, Prince RC, Harner EJ, Atlas RM. Effectiveness of bioremediation
625 fro the Exxon-Valdez oil-spill. *Nature* 1994;368:413-8.
- 626 [3] Camilli R, Reddy CM, Yoerger DR, Van Mooy BAS, Jakuba MV, Kinsey JC,
627 et al. Tracking Hydrocarbon Plume Transport and Biodegradation at
628 Deepwater Horizon. *Science* 2010;330:201-4.
- 629 [4] Zhang D, Ding A, Cui S, Hu C, Thornton SF, Dou J, et al. Whole cell
630 bioreporter application for rapid detection and evaluation of crude oil spill in
631 seawater caused by Dalian oil tank explosion. *Water Res.* 2013;47:1191-200.
- 632 [5] Peterson CH, Rice SD, Short JW, Esler D, Bodkin JL, Ballachey BE, et al.
633 Long-term ecosystem response to the Exxon Valdez oil spill. *Science*
634 2003;302:2082-6.
- 635 [6] Piatt JF, Lensink CJ, Butler W, Kendziorek M, Nysewander DR. Immediate
636 impact of the Exxon Valdez oil-spill on marine birds. *Auk* 1990;107:387-97.
- 637 [7] Van Beilen JB, Wubbolts MG, Witholt B. Genetics of alkane oxidation by
638 *Pseudomonas oleovorans*. *Biodegradation* 1994;5:161-74.
- 639 [8] Jobson A, Westlake DW, Cook FD. Microbial utilization of crude-oil. *Applied*
640 *Microbiology* 1972;23:1082-&.
- 641 [9] Becker PM, Dott W. Functional-analysis of communities of aerobic
642 heterotrophic bacteria from hydrocarbon-contaminated sites. *Microb. Ecol.*
643 1995;30:285-96.
- 644 [10] Berthe-Corti L, Fetzner S. Bacterial metabolism of n-alkanes and
645 ammonia under oxic, suboxic and anoxic conditions. *Acta Biotechnol.*
646 2002;22:299-336.
- 647 [11] Hamamura N, Fukui M, Ward DM, Inskeep WP. Assessing Soil Microbial
648 Populations Responding to Crude-Oil Amendment at Different Temperatures
649 Using Phylogenetic, Functional Gene (alkB) and Physiological Analyses.
650 *Environ. Sci. Technol.* 2008;42:7580-6.
- 651 [12] Heiss-Blanquet S, Benoit Y, Marechaux C, Monot F. Assessing the role of
652 alkane hydroxylase genotypes in environmental samples by competitive PCR.
653 *J. Appl. Microbiol.* 2005;99:1392-403.
- 654 [13] Lal B, Khanna S. Degradation of crude oil by *Acinetobacter calcoaceticus*
655 and *Alcaligenes odorans*. *J. Appl. Bacteriol.* 1996;81:355-62.
- 656 [14] Fondi M, Rizzi E, Emiliani G, Orlandini V, Berna L, Papeo MC, et al. The
657 genome sequence of the hydrocarbon-degrading *Acinetobacter venetianus*
658 VE-C3. *Res. Microbiol.* 2013;164:439-49.
- 659 [15] Hara A, Sytsubo K, Harayama S. *Alcanivorax* which prevails in
660 oil-contaminated seawater exhibits broad substrate specificity for alkane
661 degradation. *Environ. Microbiol.* 2003;5:746-53.

- 662 [16] Kasai Y, Kishira H, Sasaki T, Syutsubo K, Watanabe K, Harayama S.
663 Predominant growth of *Alcanivorax* strains in oil-contaminated and
664 nutrient-supplemented sea water. *Environ. Microbiol.* 2002;4:141-7.
- 665 [17] Sabirova JS, Ferrer M, Regenhardt D, Timmis KN, Golyshin PN.
666 Proteomic insights into metabolic adaptations in *Alcanivorax borkumensis*
667 induced by alkane utilization. *J. Bacteriol.* 2006;188:3763-73.
- 668 [18] Schneiker S, dos Santos VAPM, Bartels D, Bekel T, Brecht M, Buhrmester
669 J, et al. Genome sequence of the ubiquitous hydrocarbon-degrading marine
670 bacterium *Alcanivorax borkumensis*. *Nat. Biotechnol.* 2006;24:997-1004.
- 671 [19] Radwan SS, Sorkhoh NA, Felzmann H, ElDesouky AF. Uptake and
672 utilization of n-octacosane and n-nonacosane by *Arthrobacter nicotianae* KCC
673 B35. *J. Appl. Bacteriol.* 1996;80:370-4.
- 674 [20] Feng L, Wang W, Cheng J, Ren Y, Zhao G, Gao C, et al. Genome and
675 proteome of long-chain alkane degrading *Geobacillus thermodenitrificans*
676 NG80-2 isolated from a deep-subsurface oil reservoir. *Proc. Natl. Acad. Sci. U.*
677 *S. A.* 2007;104:5602-7.
- 678 [21] Kato T, Haruki M, Imanaka T, Morikawa M, Kanaya S. Isolation and
679 characterization of long-chain-alkane degrading *Bacillus thermoleovorans*
680 from deep subterranean petroleum reservoirs. *J. Biosci. Bioeng.*
681 2001;91:64-70.
- 682 [22] Chaerun SK, Tazaki K, Asada R, Kogure K. Bioremediation of coastal
683 areas 5 years after the Nakhodka oil spill in the Sea of Japan: isolation and
684 characterization of hydrocarbon-degrading bacteria. *Environ. Int.*
685 2004;30:911-22.
- 686 [23] Yan P. Alkane-degrading functional bacteria, its cultivation method and
687 application. CN1789408, 2006-06-21, CN20041081505 20041217,
688 CHENGDU BIOLOGY RES INST OF TH (CN) 2006.
- 689 [24] Yuste L, Corbella ME, Turiegano MJ, Karlson U, Puyet A, Rojo F.
690 Characterization of bacterial strains able to grow on high molecular mass
691 residues from crude oil processing. *FEMS Microbiol. Ecol.* 2000;32:69-75.
- 692 [25] Cravo-Laureau C, Matheron R, Cayol JL, Jouliau C, Hirschler-Rea A.
693 *Desulfatibacillum aliphaticivorans* gen. nov., sp nov., an n-alkane- and
694 n-alkene-degrading, sulfate-reducing bacterium. *Int. J. Syst. Evol. Microbiol.*
695 2004;54:77-83.
- 696 [26] Cravo-Laureau C, Grossi V, Raphel D, Matheron R, Hirschler-Rea A.
697 Anaerobic n-alkane metabolism by a sulfate-reducing bacterium,
698 *Desulfatibacillum aliphaticivorans* strain CV2803. *Appl. Environ. Microbiol.*
699 2005;71:3458-67.
- 700 [27] von der Weid I, Marques JM, Cunha CD, Lippi RK, dos Santos SCC,
701 Rosado AS, et al. Identification and biodegradation potential of a novel strain
702 of *Dietzia cinnamea* isolated from a petroleum-contaminated tropical soil. *Syst.*
703 *Appl. Microbiol.* 2007;30:331-9.
- 704 [28] Yumoto I, Nakamura A, Iwata H, Kojima K, Kusumoto K, Nodasaka Y, et al.
705 *Dietzia psychralcaliphila* sp nov., a novel, facultatively psychrophilic alkaliphile

- 706 that grows on hydrocarbons. *Int. J. Syst. Evol. Microbiol.* 2002;52:85-90.
- 707 [29] Wang L, Tang Y, Wang S, Liu R-L, Liu M-Z, Zhang Y, et al. Isolation and
708 characterization of a novel thermophilic *Bacillus* strain degrading long-chain
709 n-alkanes. *Extremophiles* 2006;10:347-56.
- 710 [30] Kotani T, Yamamoto T, Yurimoto H, Sakai Y, Kato N. Propane
711 monooxygenase and NAD(+)-dependent secondary alcohol dehydrogenase in
712 propane metabolism by *Gordonia* sp strain TY-5. *J. Bacteriol.*
713 2003;185:7120-8.
- 714 [31] Doumenq P, Aries E, Asia L, Acquaviva M, Artaud J, Gilewicz M, et al.
715 Influence of n-alkanes and petroleum on fatty acid composition of a
716 hydrocarbonoclastic bacterium: *Marinobacter hydrocarbonoclasticus* strain
717 617. *Chemosphere* 2001;44:519-28.
- 718 [32] Bonin P, Cravo-Laureau C, Michotey V, Hirschler-Rea A. The anaerobic
719 hydrocarbon biodegrading bacteria: An overview. *Ophelia* 2004;58:243-54.
- 720 [33] Churchill SA, Harper JP, Churchill PF. Isolation and characterization of a
721 *Mycobacterium* species capable of degrading three- and four-ring aromatic
722 and aliphatic hydrocarbons. *Appl. Environ. Microbiol.* 1999;65:549-52.
- 723 [34] van Beilen JB, Smits THM, Whyte LG, Schorcht S, Rothlisberger M,
724 Plaggemeier T, et al. Alkane hydroxylase homologues in Gram-positive strains.
725 *Environ. Microbiol.* 2002;4:676-82.
- 726 [35] Zhang HM, Kallimanis A, Koukkou AI, Drainas C. Isolation and
727 characterization of novel bacteria degrading polycyclic aromatic hydrocarbons
728 from polluted Greek soils. *Appl. Microbiol. Biotechnol.* 2004;65:124-31.
- 729 [36] Engelhardt MA, Daly K, Swannell RPJ, Head IM. Isolation and
730 characterization of a novel hydrocarbon-degrading, Gram-positive bacterium,
731 isolated from intertidal beach sediment, and description of *Planococcus*
732 *alkanoclasticus* sp nov. *J. Appl. Microbiol.* 2001;90:237-47.
- 733 [37] Koch AK, Kappeli O, Fiechter A, Reiser J. Hydrocarbon assimilatin and
734 biofurfactant production in *Pseudomonas-Aeruginosa* mutants. *J. Bacteriol.*
735 1991;173:4212-9.
- 736 [38] Naik PR, Sakthivel N. Functional characterization of a novel
737 hydrocarbonoclastic *Pseudomonas* sp strain PUP6 with
738 plant-growth-promoting traits and antifungal potential. *Res. Microbiol.*
739 2006;157:538-46.
- 740 [39] Kunihiro N, Haruki M, Takano K, Morikawa M, Kanaya S. Isolation and
741 characterization of *Rhodococcus* sp strains TNP2 and T12 that degrade
742 2,6,10,14-tetramethylpentadecane (pristane) at moderately low temperatures.
743 *J. Biotechnol.* 2005;115:129-36.
- 744 [40] Andreoni V, Bernasconi S, Colombo M, van Beilen JB, Cavalca L.
745 Detection of genes for alkane and naphthalene catabolism in *Rhodococcus* sp
746 strain 1BN. *Environ. Microbiol.* 2000;2:572-7.
- 747 [41] Zarilla KA, Perry JJ. *Thermoleophilum album* gen. nov. and sp. nov., a
748 bacterium obligate for thermophily and normal-alkane substrates. *Arch.*
749 *Microbiol.* 1984;137:286-90.

- 750 [42] Wang W, Shao Z. Enzymes and genes involved in aerobic alkane
751 degradation. *Front. Microbiol.* 2013;4.
- 752 [43] Jurelevicius D, Alvarez VM, Peixoto R, Rosado AS, Seldin L. The use of a
753 combination of *alkB* primers to better characterize the distribution of
754 alkane-degrading bacteria. *PLoS One* 2013;8.
- 755 [44] Smits THM, Balada SB, Witholt B, van Beilen JB. Functional analysis of
756 alkane hydroxylases from gram-negative and gram-positive bacteria. *J.*
757 *Bacteriol.* 2002;184:1733-42.
- 758 [45] Amouric A, Quemeneur M, Grossi V, Liebgott PP, Auria R, Casalot L.
759 Identification of different alkane hydroxylase systems in *Rhodococcus ruber*
760 strain SP2B, an hexane-degrading actinomycete. *J. Appl. Microbiol.*
761 2010;108:1903-16.
- 762 [46] Whyte LG, Hawari J, Zhou E, Bourbonniere L, Inniss WE, Greer CW.
763 Biodegradation of variable-chain-length alkanes at low temperatures by a
764 psychrotrophic *Rhodococcus* sp. *Appl. Environ. Microbiol.* 1998;64:2578-84.
- 765 [47] Whyte LG, Smits THM, Labbe D, Witholt B, Greer CW, van Beilen JB.
766 Gene cloning and characterization of multiple alkane hydroxylase systems in
767 *Rhodococcus* strains Q15 and NRRL B-16531. *Appl. Environ. Microbiol.*
768 2002;68:5933-42.
- 769 [48] Razak CNA, Wang WF, Rahman S, Basri M, Salleh AB. Isolation of the
770 crude oil degrading marine *Acinetobacter* sp E11. *Acta Biotechnol.*
771 1999;19:213-23.
- 772 [49] Pleshakova EV, Muratova AY, Turkovskaya OV. Degradation of mineral oil
773 with a strain of *Acinetobacter calcoaceticus*. *Appl Biochem Micro+*
774 2001;37:342-7.
- 775 [50] DiCello F, Pepi M, Baldi F, Fani R. Molecular characterization of an
776 n-alkane-degrading bacterial community and identification of a new species,
777 *Acinetobacter venetianus*. *Res. Microbiol.* 1997;148:237-49.
- 778 [51] Tanaka D, Takashima M, Mizuta A, Tanaka S, Sakatoku A, Nishikawa A, et
779 al. *Acinetobacter* sp Ud-4 Efficiently Degrades Both Edible and Mineral Oils:
780 Isolation and Characterization. *Curr. Microbiol.* 2010;60:203-9.
- 781 [52] Kennedy RS, Finnerty WR, Sudarsanan K, Young RA. Microbial
782 assimilation of hydrocarbons. 1. Fine-structure of a hydrocarbon oxidizing
783 *Acinetobacter* sp. *Arch. Microbiol.* 1975;102:75-83.
- 784 [53] Bajpai U, Kuhad RC, Khanna S. Mineralization of (14)C octadecane by
785 *Acinetobacter calcoaceticus* S19. *Can. J. Microbiol.* 1998;44:681-6.
- 786 [54] van Beilen JB, Li Z, Duetz WA, Smits THM, Witholt B. Diversity of alkane
787 hydroxylase systems in the environment. *Oil & Gas Science and*
788 *Technology-Revue D Ifp Energies Nouvelles* 2003;58:427-40.
- 789 [55] Viggor S, Joesaar M, Vedler E, Kiiker R, Parnpuu L, Heinaru A.
790 Occurrence of diverse alkane hydroxylase *alkB* genes in indigenous
791 oil-degrading bacteria of Baltic Sea surface water. *Mar. Pollut. Bull.*
792 2015;101:507-16.
- 793 [56] Muyzer G, Dewaal EC, Uitterlinden AG. Profiling of complex microbial

- 794 populations by denaturing gradient gel electrophoresis analysis of polymerase
795 chain reaction-amplified genes coding for 16S rRNA. *Appl. Environ. Microbiol.*
796 1993;59:695-700.
- 797 [57] Tringe SG, von Mering C, Kobayashi A, Salamov AA, Chen K, Chang HW,
798 et al. Comparative metagenomics of microbial communities. *Science*
799 2005;308:554-7.
- 800 [58] Lindstrom JE, Barry RP, Braddock JF. Long-term effects on microbial
801 communities after a subarctic oil spill. *Soil Biol. Biochem.* 1999;31:1677-89.
- 802 [59] Aislabie JM, Balks MR, Foght JM, Waterhouse EJ. Hydrocarbon spills on
803 Antarctic soils: Effects and management. *Environ. Sci. Technol.*
804 2004;38:1265-74.
- 805 [60] Powell SM, Bowman JP, Snape I, Stark JS. Microbial community variation
806 in pristine and polluted nearshore Antarctic sediments. *FEMS Microbiol. Ecol.*
807 2003;45:135-45.
- 808 [61] Yakimov MM, Denaro R, Genovese M, Cappello S, D'Auria G, Chernikova
809 TN, et al. Natural microbial diversity in superficial sediments of Milazzo Harbor
810 (Sicily) and community successions during microcosm enrichment with various
811 hydrocarbons. *Environ. Microbiol.* 2005;7:1426-41.
- 812 [62] Maila MP, Randima P, Dronen K, Cloete TE. Soil microbial communities:
813 Influence of geographic location and hydrocarbon pollutants. *Soil Biol.*
814 *Biochem.* 2006;38:303-10.
- 815 [63] Liang YT, Van Nostrand JD, Deng Y, He ZL, Wu LY, Zhang X, et al.
816 Functional gene diversity of soil microbial communities from five
817 oil-contaminated fields in China. *ISME J.* 2011;5:403-13.
- 818 [64] Cheung PY, Kinkle BK. Mycobacterium diversity and pyrene mineralization
819 in petroleum-contaminated soils. *Appl. Environ. Microbiol.* 2001;67:2222-9.
- 820 [65] Liang YT, Zhang X, Zhou JZ, Li GH. Long-term oil contamination
821 increases deterministic assembly processes in soil microbes. *Ecol. Appl.*
822 2015;25:1235-43.
- 823 [66] Juck D, Charles T, Whyte LG, Greer CW. Polyphasic microbial community
824 analysis of petroleum hydrocarbon-contaminated soils from two northern
825 Canadian communities. *FEMS Microbiol. Ecol.* 2000;33:241-9.
- 826 [67] Al-Saleh E, Akbar A. Occurrence of *Pseudomonas aeruginosa* in Kuwait
827 soil. *Chemosphere* 2015;120:100-7.
- 828 [68] Sorkhoh NA, Ghannoum MA, Ibrahim AS, Stretton RJ, Radwan SS. Crude
829 oil and hydrocarbon-degrading strains of *Rhodococcus rhodochromus* isolated
830 from soil and marine environments in Kuwait. *Environ. Pollut.* 1990;65:1-17.
- 831 [69] Pi YR, Meng L, Bao MT, Sun PY, Lu JR. Degradation of crude oil and
832 relationship with bacteria and enzymatic activities in laboratory testing. *Int.*
833 *Biodeterior. Biodegrad.* 2016;106:106-16.
- 834 [70] Abed RMM, Safi NMD, Koster J, de Beer D, El-Nahhal Y, Rullkotter J, et al.
835 Microbial diversity of a heavily polluted microbial mat and its community
836 changes following degradation of petroleum compounds. *Appl. Environ.*
837 *Microbiol.* 2002;68:1674-83.

- 838 [71] Margesin R, Labbe D, Schinner F, Greer CW, Whyte LG. Characterization
839 of hydrocarbon-degrading microbial populations in contaminated and pristine
840 alpine soils. *Appl. Environ. Microbiol.* 2003;69:3085-92.
- 841 [72] Roling WFM, Milner MG, Jones DM, Lee K, Daniel F, Swannell RJP, et al.
842 Robust hydrocarbon degradation and dynamics of bacterial communities
843 during nutrient-enhanced oil spill bioremediation. *Appl. Environ. Microbiol.*
844 2002;68:5537-48.
- 845 [73] Bento FM, Camargo FAO, Okeke BC, Frankenberger WT. Comparative
846 bioremediation of soils contaminated with diesel oil by natural attenuation,
847 biostimulation and bioaugmentation. *Bioresour. Technol.* 2005;96:1049-55.
- 848 [74] Lin Z, Zhen Z, Wu Z, Yang J, Zhong L, Hu H, et al. The impact on the soil
849 microbial community and enzyme activity of two earthworm species during the
850 bioremediation of pentachlorophenol-contaminated soils. *J. Hazard. Mater.*
851 2016;301:35-45.
- 852 [75] McKew BA, Coulon F, Yakimov MM, Denaro R, Genovese M, Smith CJ, et
853 al. Efficacy of intervention strategies for bioremediation of crude oil in marine
854 systems and effects on indigenous hydrocarbonoclastic bacteria. *Environ.*
855 *Microbiol.* 2007;9:1562-71.
- 856 [76] Tahhan RA, Ammari TG, Goussous SJ, Al-Shdaifat HI. Enhancing the
857 biodegradation of total petroleum hydrocarbons in oily sludge by a modified
858 bioaugmentation strategy. *Int. Biodeterior. Biodegrad.* 2011;65:130-4.
- 859 [77] Tyagi M, da Fonseca MMR, de Carvalho CCCR. Bioaugmentation and
860 biostimulation strategies to improve the effectiveness of bioremediation
861 processes. *Biodegradation* 2011;22:231-41.
- 862 [78] El Fantroussi S, Agathos SN. Is bioaugmentation a feasible strategy for
863 pollutant removal and site remediation? *Curr. Opin. Microbiol.* 2005;8:268-75.
- 864 [79] Thompson IP, van der Gast CJ, Ciric L, Singer AC. Bioaugmentation for
865 bioremediation: the challenge of strain selection. *Environ. Microbiol.*
866 2005;7:909-15.
- 867 [80] vanVeen JA, vanOverbeek LS, vanElsas JD. Fate and activity of
868 microorganisms introduced into soil. *Microbiol. Mol. Biol. Rev.* 1997;61:121-&.
- 869 [81] Vogel TM. Bioaugmentation as a soil bioremediation approach. *Curr. Opin.*
870 *Biotechnol.* 1996;7:311-6.
- 871 [82] Karamalidis AK, Evangelou AC, Karabika E, Koukkou AI, Drinas C,
872 Voudrias EA. Laboratory scale bioremediation of petroleum-contaminated soil
873 by indigenous microorganisms and added *Pseudomonas aeruginosa* strain
874 Spet. *Bioresour. Technol.* 2010;101:6545-52.
- 875 [83] Kaeberlein T, Lewis K, Epstein SS. Isolating "uncultivable"
876 microorganisms in pure culture in a simulated natural environment. *Science*
877 2002;296:1127-9.
- 878 [84] Radajewski S, Ineson P, Parekh NR, Murrell JC. Stable-isotope probing as
879 a tool in microbial ecology. *Nature* 2000;403:646-9.
- 880 [85] Uhlik O, Wald J, Strejcek M, Musilova L, Ridl J, Hroudova M, et al.
881 Identification of Bacteria Utilizing Biphenyl, Benzoate, and Naphthalene in

- 882 Long-Term Contaminated Soil. *PLoS One* 2012;7.
- 883 [86] Song M, Luo C, Jiang L, Zhang D, Wang Y, Zhang G. Identification of
884 Benzo a pyrene-Metabolizing Bacteria in Forest Soils by Using DNA-Based
885 Stable-Isotope Probing. *Appl. Environ. Microbiol.* 2015;81:7368-76.
- 886 [87] Chen Y, Murrell JC. When metagenomics meets stable-isotope probing:
887 progress and perspectives. *Trends Microbiol.* 2010;18:157-63.
- 888 [88] Zhang D, Berry JP, Zhu D, Wang Y, Chen Y, Jiang B, et al. Magnetic
889 nanoparticle-mediated isolation of functional bacteria in a complex microbial
890 community. *The ISME Journal* 2015;9:603-14.
- 891 [89] Zhao X, Li H, Ding A, Zhou G, Sun Y, Zhang D. Preparing and
892 characterizing Fe₃O₄@cellulose nanocomposites for effective isolation of
893 cellulose-decomposing microorganisms. *Mater. Lett.* 2016;163:154-7.
- 894 [90] Zhang D, Fakhrullin RF, Özmen M, Wang H, Wang J, Paunov VN, et al.
895 Functionalization of whole-cell bacterial reporters with magnetic nanoparticles.
896 *Microbial Biotech.* 2011;4:89-97.
- 897 [91] Herlemann DPR, Labrenz M, Juergens K, Bertilsson S, Waniek JJ,
898 Andersson AF. Transitions in bacterial communities along the 2000 km salinity
899 gradient of the Baltic Sea. *ISME J.* 2011;5:1571-9.
- 900 [92] Smits THM, Rothlisberger M, Witholt B, van Beilen JB. Molecular
901 screening for alkane hydroxylase genes in Gram-negative and Gram-positive
902 strains. *Environ. Microbiol.* 1999;1:307-17.
- 903 [93] Kuhn E, Bellicanta GS, Pellizari VH. New alk genes detected in Antarctic
904 marine sediments. *Environ. Microbiol.* 2009;11:669-73.
- 905 [94] Marchant R, Sharkey FH, Banat IM, Rahman TJ, Perfumo A. The
906 degradation of n-hexadecane in soil by thermophilic geobacilli. *FEMS*
907 *Microbiol. Ecol.* 2006;56:44-54.
- 908 [95] Zhang J, Kobert K, Flouri T, Stamatakis A. PEAR: a fast and accurate
909 Illumina Paired-End reAd mergeR. *Bioinformatics* 2014;30:614-20.
- 910 [96] Hueso S, García C, Hernández T. Severe drought conditions modify the
911 microbial community structure, size and activity in amended and unamended
912 soils. *Soil Biology and Biochemistry* 2012;50:167-73.
- 913 [97] Tang J, Wang R, Niu X, Zhou Q. Enhancement of soil petroleum
914 remediation by using a combination of ryegrass (*Lolium perenne*) and different
915 microorganisms. *Soil and Tillage Research* 2010;110:87-93.
- 916 [98] Fryirs KA, Hafsteinsdóttir EG, Stark SC, Gore DB. Metal and petroleum
917 hydrocarbon contamination at Wilkes Station, East Antarctica. *Antarct. Sci.*
918 2014;27:118-33.
- 919 [99] Zhang D, He Y, Wang Y, Wang H, Wu L, Aries E, et al. Whole-cell bacterial
920 bioreporter for actively searching and sensing of alkanes and oil spills.
921 *Microbial Biotech.* 2012;5:87-97.
- 922 [100] Li C, Zhang D, Song Y, Jiang B, Li G, Huang WE. Whole cell bioreporter
923 for the estimation of oil contamination. *Environ. Eng. Manage. J.*
924 2013;12:1353-8.
- 925 [101] Zhang D, Zhao Y, He Y, Wang Y, Zhao Y, Zheng Y, et al. Characterization

- 926 and modeling of transcriptional cross-regulation in *Acinetobacter baylyi* ADP1.
927 ACS Synthetic Biology 2012;1:274-83.
- 928 [102] Al-Anizi AA, Hellyer MT, Zhang D. Toxicity assessment and modelling of
929 Moringa oleifera seeds in water purification by whole cell bioreporter. Water
930 Res. 2014;56:77-87.
- 931 [103] Xu Y, Li C, Zhu X, Huang WE, Zhang D. Application of magnetic
932 nanoparticles in drinking water purification. Environ. Eng. Manage. J.
933 2014;13:2023-9.
- 934 [104] Lin Z, Xu Y, Zhen Z, Fu Y, Liu Y, Li W, et al. Application and reactivation of
935 magnetic nanoparticles in *Microcystis aeruginosa* harvesting. Bioresour.
936 Technol. 2015;190:82-8.
- 937 [105] Chen C, Zhang D, Thornton SF, Duan M, Luo Y, Ding A, et al.
938 Functionalization and immobilization of whole cell bioreporters for the
939 detection of environmental contamination. Environ. Eng. Manage. J.
940 2013;12:1417-22.
- 941 [106] Pond KL, Huang YS, Wang Y, Kulpa CF. Hydrogen isotopic composition
942 of individual n-alkanes as an intrinsic tracer for bioremediation and source
943 identification of petroleum contamination. Environ. Sci. Technol.
944 2002;36:724-8.
- 945 [107] Hamamura N, Olson SH, Ward DM, Inskeep WP. Microbial population
946 dynamics associated with crude-oil biodegradation in diverse soils. Appl.
947 Environ. Microbiol. 2006;72:6316-24.
- 948 [108] Chaineau CH, Rougeux G, Yepremian C, Oudot J. Effects of nutrient
949 concentration on the biodegradation of crude oil and associated microbial
950 populations in the soil. Soil Biol. Biochem. 2005;37:1490-7.
- 951 [109] Caldwell ME, Garrett RM, Prince RC, Suflita JM. Anaerobic
952 biodegradation of long-chain n-alkanes under sulfate-reducing conditions.
953 Environ. Sci. Technol. 1998;32:2191-5.
- 954 [110] Hasinger M, Scherr KE, Lundaa T, Braeuer L, Zach C, Loibner AP.
955 Changes in iso- and n-alkane distribution during biodegradation of crude oil
956 under nitrate and sulphate reducing conditions. J. Biotechnol. 2012;157:490-8.
- 957 [111] Smith CB, Tolar BB, Hollibaugh JT, King GM. Alkane hydroxylase gene
958 (alkB) phylotype composition and diversity in northern Gulf of Mexico
959 bacterioplankton. Front. Microbiol. 2013;4.
- 960 [112] Yang S, Wen X, Zhao L, Shi Y, Jin H. Crude Oil Treatment Leads to Shift
961 of Bacterial Communities in Soils from the Deep Active Layer and Upper
962 Permafrost along the China-Russia Crude Oil Pipeline Route. PLoS One
963 2014;9.
- 964 [113] Alonso-Gutierrez J, Figueras A, Albaiges J, Jimenez N, Vinas M, Solanas
965 AM, et al. Bacterial Communities from Shoreline Environments (Costa da
966 Morte, Northwestern Spain) Affected by the Prestige Oil Spill. Appl. Environ.
967 Microbiol. 2009;75:3407-18.
- 968 [114] Mattes TE, Alexander AK, Richardson PM, Munk AC, Han CS, Stothard P,
969 et al. The genome of Polaromonas sp strain JS666: Insights into the evolution

- 970 of a hydrocarbon- and xenobiotic-degrading bacterium, and features of
971 relevance to biotechnology. *Appl. Environ. Microbiol.* 2008;74:6405-16.
- 972 [115] van Beilen JB, Panke S, Lucchini S, Franchini AG, Rothlisberger M,
973 Witholt B. Analysis of *Pseudomonas putida* alkane-degradation gene clusters
974 and flanking insertion sequences: evolution and regulation of the alk genes.
975 *Microbiology-SGM* 2001;147:1621-30.
- 976 [116] Giebler J, Wick LY, Chatzinotas A, Harms H. Alkane-degrading bacteria
977 at the soil-litter interface: comparing isolates with T-RFLP-based community
978 profiles. *FEMS Microbiol. Ecol.* 2013;86:45-58.
- 979 [117] Lang FS, Destain J, Delvigne F, Druart P, Ongena M, Thonart P.
980 Characterization and Evaluation of the Potential of a Diesel-Degrading
981 Bacterial Consortium Isolated from Fresh Mangrove Sediment. *Water Air Soil*
982 *Pollut.* 2016;227.
- 983 [118] Aburto-Medina A, Adetutu EM, Aloor S, Weber J, Patil SS, Sheppard PJ,
984 et al. Comparison of indigenous and exogenous microbial populations during
985 slurry phase biodegradation of long-term hydrocarbon-contaminated soil.
986 *Biodegradation* 2012;23:813-22.
- 987 [119] Hassanshahian M, Bayat Z, Cappello S, Smedile F, Yakimov M.
988 Comparison the effects of bioaugmentation versus biostimulation on marine
989 microbial community by PCR-DGGE: A mesocosm scale. *Journal of*
990 *Environmental Sciences* 2016;43:136-46.
- 991 [120] Tyagi M, da Fonseca MMR, de Carvalho C. Bioaugmentation and
992 biostimulation strategies to improve the effectiveness of bioremediation
993 processes. *Biodegradation* 2011;22:231-41.
- 994 [121] Byers JE. Impact of non-indigenous species on natives enhanced by
995 anthropogenic alteration of selection regimes. *Oikos* 2002;97:449-58.
- 996 [122] Gallego JLR, Loredó J, Llamas JF, Vazquez F, Sanchez J.
997 Bioremediation of diesel-contaminated soils: Evaluation of potential in situ
998 techniques by study of bacterial degradation. *Biodegradation* 2001;12:325-35.
- 999 [123] Ruberto L, Vazquez SC, Mac Cormack WP. Effectiveness of the natural
1000 bacterial flora, biostimulation and bioaugmentation on the bioremediation of a
1001 hydrocarbon contaminated Antarctic soil. *Int. Biodeterior. Biodegrad.*
1002 *2003;52:115-25.*
- 1003 [124] Margesin R, Schinner F. Efficiency of indigenous and inoculated
1004 cold-adapted soil microorganisms for biodegradation of diesel oil in Alpine soils.
1005 *Appl. Environ. Microbiol.* 1997;63:2660-4.
- 1006 [125] Kauppi S, Sinkkonen A, Romantschuk M. Enhancing bioremediation of
1007 diesel-fuel-contaminated soil in a boreal climate: Comparison of biostimulation
1008 and bioaugmentation. *Int. Biodeterior. Biodegrad.* 2011;65:359-68.
- 1009 [126] Sajna KV, Sukumaran RK, Gottumukkala LD, Pandey A. Crude oil
1010 biodegradation aided by biosurfactants from *Pseudozyma* sp NII 08165 or its
1011 culture broth. *Bioresour. Technol.* 2015;191:133-9.
- 1012 [127] Rahman KSM, Rahman TJ, Kourkoutas Y, Petsas I, Marchant R, Banat
1013 IM. Enhanced bioremediation of n-alkane in petroleum sludge using bacterial

1014 consortium amended with rhamnolipid and micronutrients. Bioresour. Technol.
1015 2003;90:159-68.
1016
1017
1018
1019
1020

ACCEPTED MANUSCRIPT

1021

1022 **Figure captions**

1023 **Fig. 1.** Soil magnetic functionalization efficiency against the ratio of soil to
1024 MNPs (0.066 to 19,500, w/w).

1025 **Fig. 2.** The n-alkane degradation curve in soils functionalized with/without
1026 MNPs (A). KKN (\square) and CKP (\blacksquare) represent the original soil treatments without/
1027 with n-alkane amendment. MNPN (\circ) and MNPP (\bullet) refer to the treatments of
1028 MNPs-functionalized soils without/with n-alkane amendment. Change of
1029 individual n-alkanes with specific carbon chain length (B). The abundance of
1030 each n-alkane (C_{10} - C_{24}) is normalized as 100% for original mineral oil.

1031 **Fig. 3.** Relative abundance of soil bacteria at the family level (A), Bray-Curtis
1032 cluster (B) and PCoA (C) analysis for soil samples amended with/without
1033 n-alkane at different time points. Taxonomic assignment was carried out with
1034 the Greengenes 16S rRNA database. NC refers to the original soils (day 0);
1035 “_20” and “_40” mean the DNA collected on days 20 and 40, respectively; KKN
1036 and MNPN represent soil DNA of treatments without n-alkane
1037 amendment; CKP and MNPP are soil DNA of treatments with n-alkane
1038 amendment; MFCN and MFCP represent DNA in magnetic-free cell (MFC)
1039 fractions from MNPN and MNPP treatments.

1040 **Fig. 4.** Quantification of 16S rRNA and n-alkane monooxygenase genes in
1041 different treatments. (A): 16S rRNA abundance against incubation time, where
1042 y-axis represents the 16S rRNA copies/mL. (B), (C) and (D): relative
1043 abundance of n-alkane monooxygenase gene (alkA/16S, alkP/16S and
1044 alkR/16S) against incubation time.

1045 **Fig. 5.** Phenotypic microarray profiling of magnetic free cells (MFCs).
1046 Respiration level of PM01 (carbon sources) plates for MFCN (A) and MFCP
1047 (B). Respiration level and n-alkane degradation rate of PM03 (nitrogen
1048 sources) plates for MFCN (C) and MFCP (D), with n-alkane mixtures as
1049 sole carbon source.

1050 **Fig. 6.** Correlation analysis of microbial respiration level and n-alkane
1051 degradation rate in phenotypic microarray. Red and white circles represent the
1052 data of MFCP and MFCN, respectively.

1053

Table

Table 1. Primers and amplification programs.

Target	Name	5'-3'	Heating			Amplification						Reference
			Temp (°C)	Time (s)	Cycle	Denaturation		Annealing		Extension		
						Temp (°C)	Time (s)	Temp (°C)	Time (s)	Temp (°C)	Time (s)	
Total bacteria	alk_R F/alk_ RR	CCTACGGGNGGCWGCAG/TACNV GGGTATCTAATCC	95	240	30	95	45	40	60	72	300	[91]
n-Alkane mono-oxygenase gene	alk_P F/alk_ PR	ATCTGGGCGCGTTGGGATTTGAG CG/CGCATGGTGATCGCTGTGCCG CTGC	94	180	30	94	60	45	60	72	60	[92]
	alk_A F/alk_ AR	GCICAIARITIRKICAYAA/GCITGITGI TCISWRTGICGYTG	94	180	30	94	60	58.5	30	72	30	[93]
	alk_R F/alk_ RR	GGTACGGSCAYTTCTACRTC GA/C GGRTTCGCGTGRTGRT	94	180	34	94	45	52	45	72	45	[94]

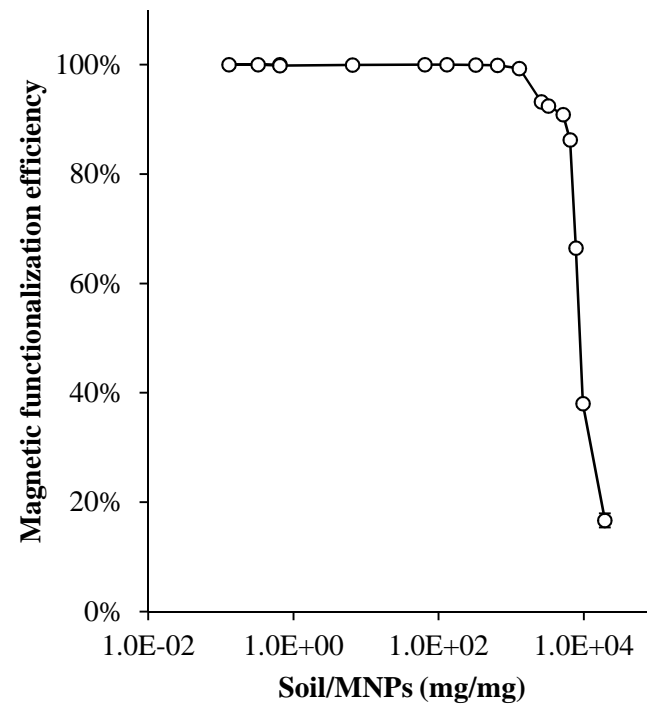
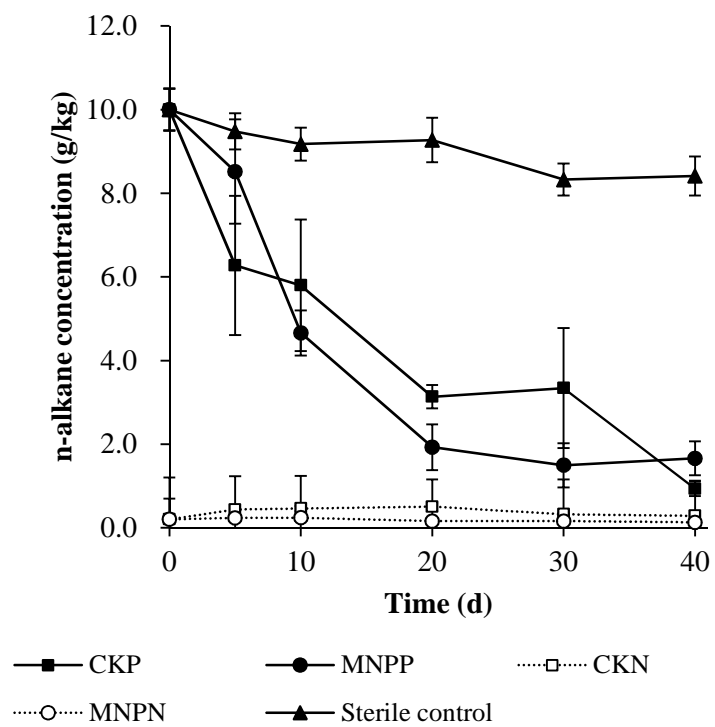
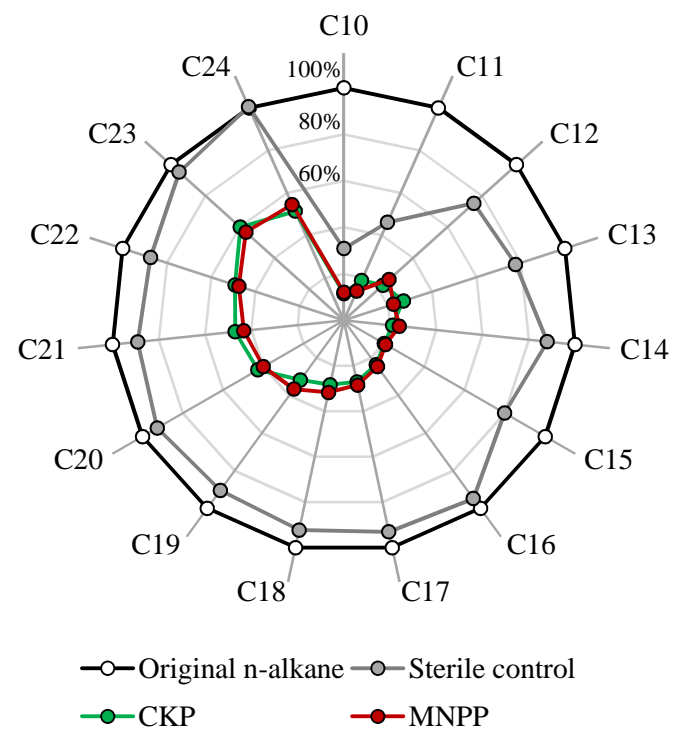


Figure 1



(A)



(B)

Figure 2

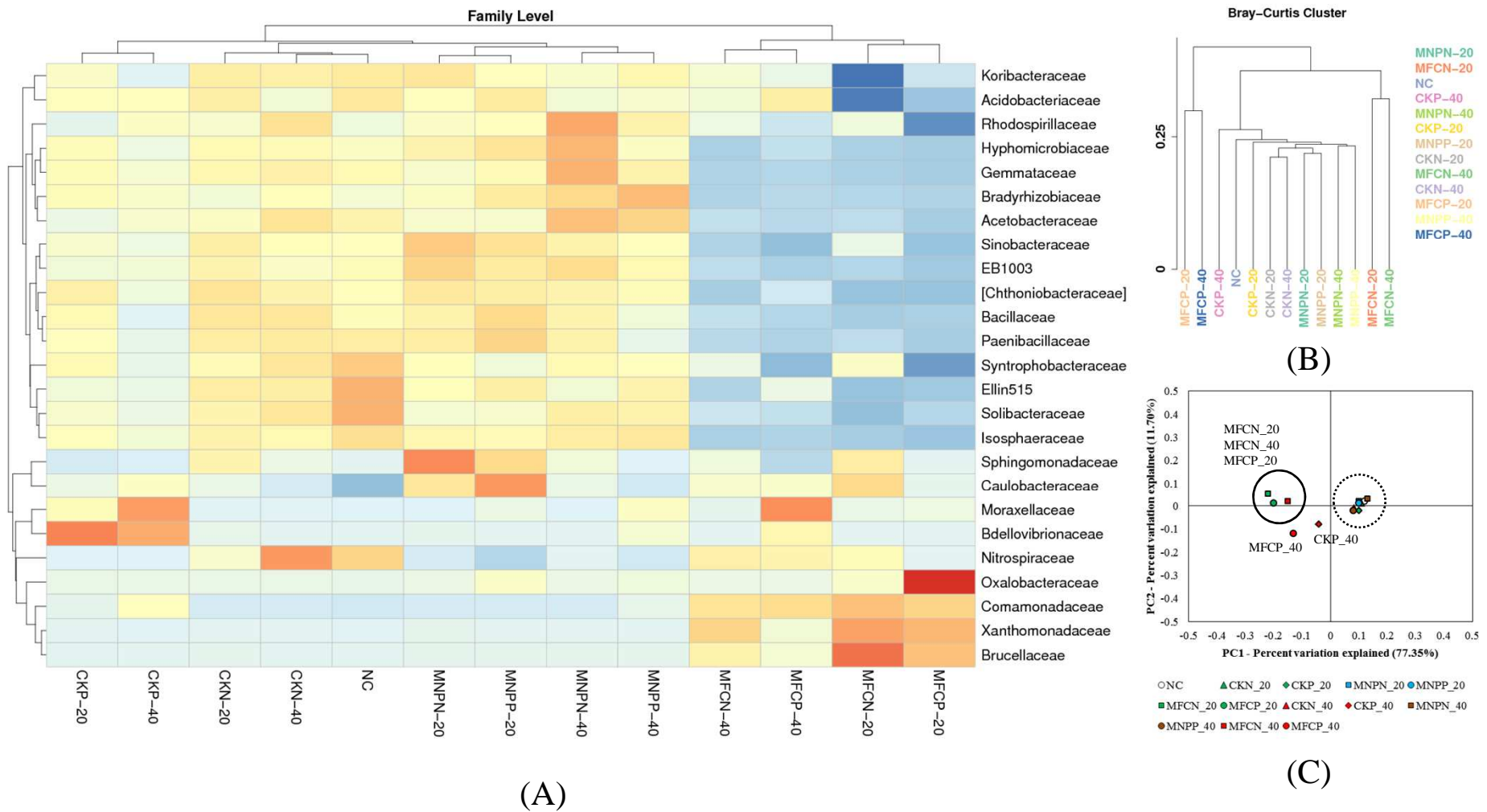
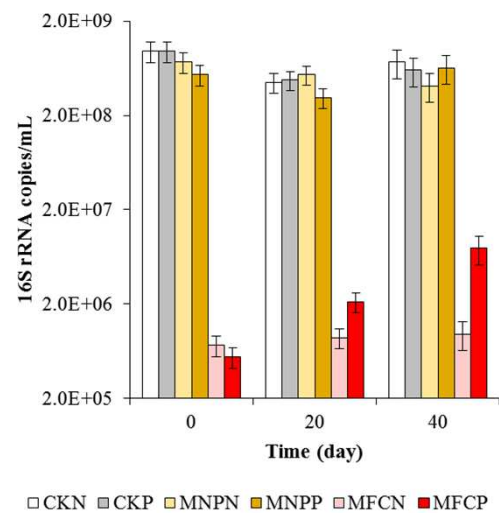
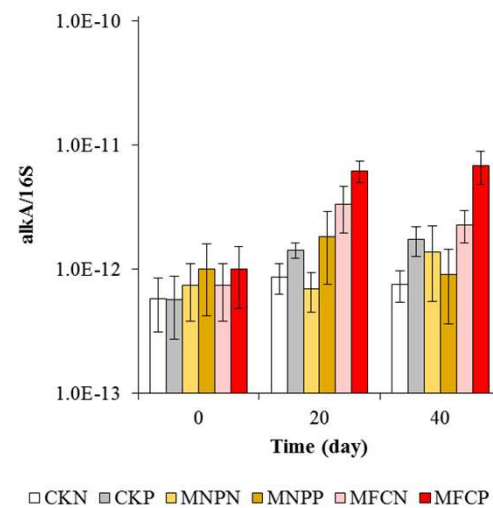


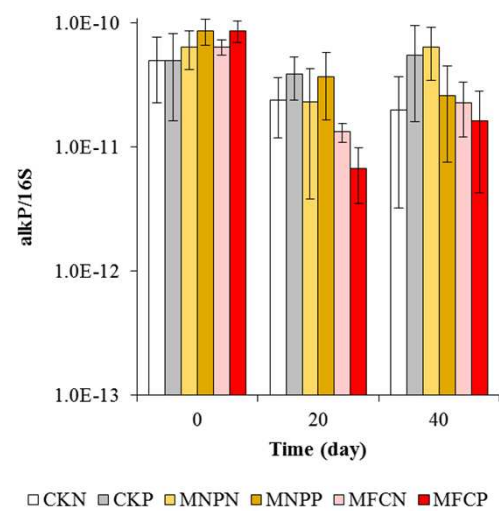
Figure 3



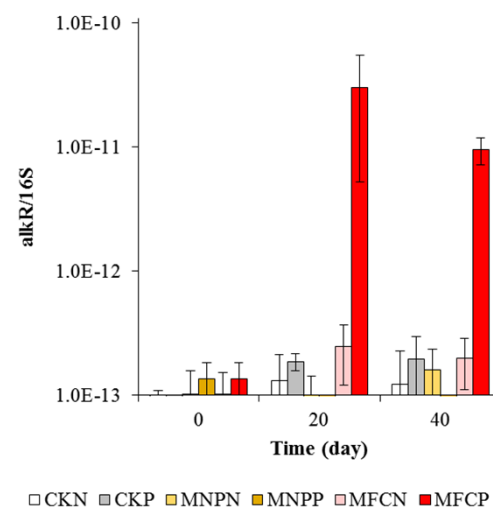
(A)



(B)



(C)



(D)

Figure 4

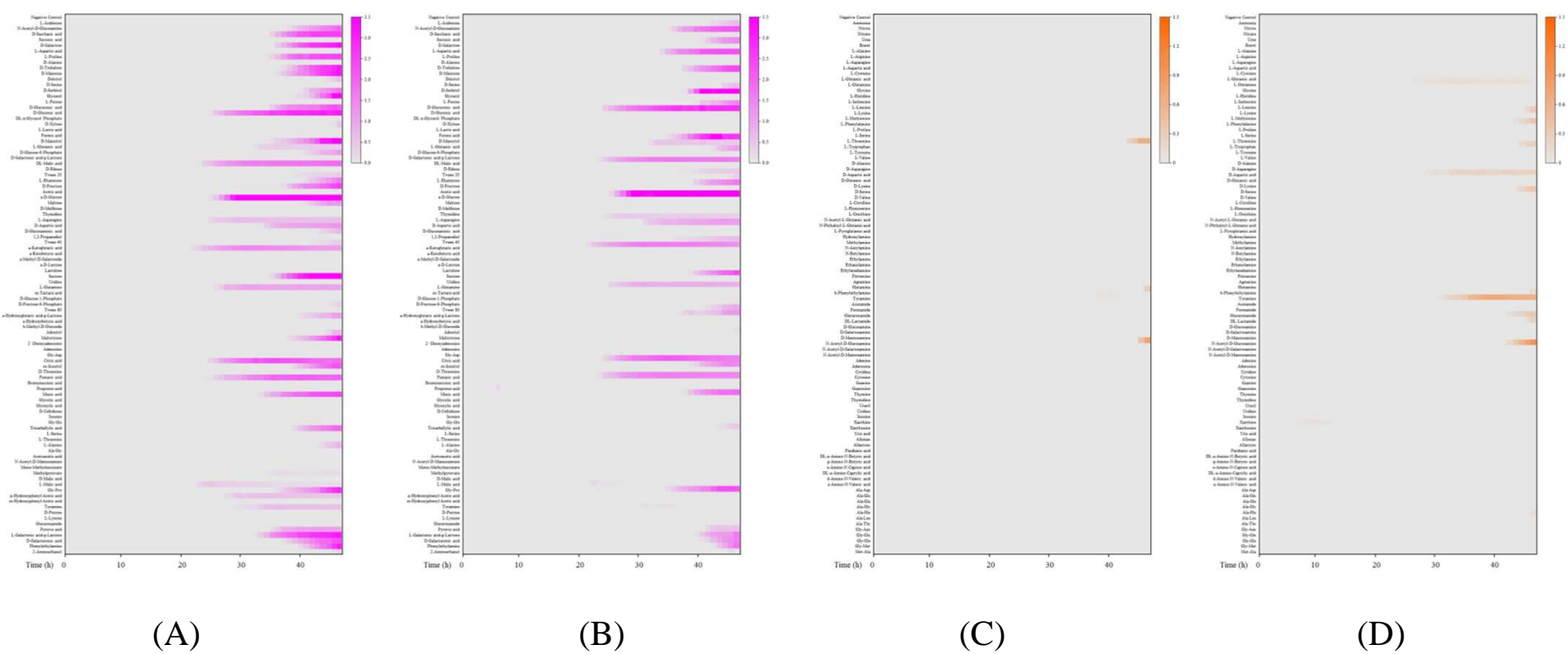


Figure 5

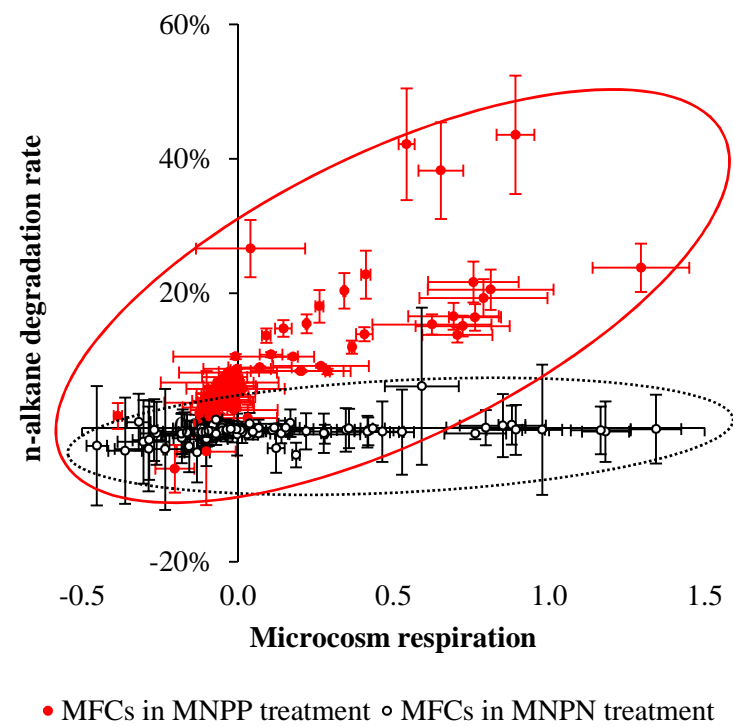


Figure 6